

# 17C.7 ANALYSIS OF SHEAR-RELATIVE ASYMMETRIES IN TROPICAL CYCLONE EYEWALL SLOPE

Andrew T. Hazelton\*<sup>1</sup>, Robert Rogers<sup>2</sup>, and Robert E. Hart<sup>1</sup>

<sup>1</sup> *The Florida State University, Tallahassee, FL*

<sup>2</sup> *NOAA/AOML/Hurricane Research Division, Miami, FL*

## 1. INTRODUCTION

Tropical Cyclone (TC) eyewall slope has recently been analyzed observationally by Stern and Nolan (2009, 2014), who quantified the slope of the azimuthal mean Radius of Maximum Winds (RMW) for several TCs using airborne velocity data, and Hazelton and Hart (2013), who analyzed azimuthal mean slope of the 20 dBZ contour for 15 different TCs using airborne radar reflectivity data. However, neither of these studies analyzed azimuthal variation in slope

There have been a couple of case studies that have briefly looked at asymmetries in eyewall slope across the eyewall due to shear. Specifically, Halverson et al. (2006) noted an apparent along-shear difference in slope across the eyewall in Hurricane Erin (2001). Rogers and Uhlhorn (2008) used flight-level and SFMR data to calculate lower-troposphere eyewall slope in Hurricane Rita, and showed that the slope asymmetry across the eyewall seemed to increase as shear increased. However, neither of these studies quantified shear-relative variation in slope for multiple TCs, and only Rogers and Uhlhorn (2008) briefly touched on the connection between asymmetry and shear magnitude.

Accordingly, in this study, we make use of airborne Doppler Radar reflectivity and velocity data to analyze the azimuthal variation of several metrics of TC eyewall slope in a shear-relative framework, building off of previous analysis of the structure of sheared TCs.

## 2. DATA AND METHODOLOGY

In this study, we use the 3-dimensional Doppler Radar composites from the NOAA-P3. The horizontal resolution is 2 km, and the vertical resolution is 0.5 km. Only cases with sufficient azimuthal coverage around the eyewall were included in the dataset.

For the shear magnitude and direction we used the data from the SHIPS archive. The shear vector is obtained from the Global Forecast System (GFS) analyses by removing the TC vortex and then averaging the 850-200 hPa shear over a radius from 0-500 km relative to the storm center, and is available for the six-hourly synoptic times (00 UTC, 06 UTC, 12 UTC, 18 UTC).

Hazelton and Hart (2013) analyzed azimuthal mean slope of the 20 dBZ contour, while Stern and Nolan (2009) looked at RMW slope and the slope of an angular momentum surface. Here, we analyze azimuthal variation in all three slope metrics. The slopes of the RMW and M surface are likely to show more variation due to the influence of shear on vortex structure, while

---

\*Corresponding Author Address: Andrew T. Hazelton, Department of Earth, Ocean, and Atmospheric Science, the Florida State University, Tallahassee, FL, 32306-4520

Email: ath09c@my.fsu.edu

dBZ slope likely shows more of the influence of convection due to shear.

The cases in the radar dataset suitable for this analysis were selected using the following criteria:

1. Only TCs with wind speed greater than 33 m/s (hurricane intensity)
2. Only TCs more than 50 km from land
3. Only cases with sufficient azimuthal coverage in all 4 shear-relative quadrants
4. Only cases where the 20 dBZ surface and RMW were located at the same eyewall (there were a few cases with secondary eyewalls that had to be removed for this reason).

The data used after these filters consist of 36 flights into 15 different TCs from 1997-2010.

### 3. RESULTS

#### a. Overall Shear-Relative Variation

Figures 1a-b show the azimuthal variation of RMW and M slope for the 36 cases analyzed in the study. For RMW slope, the two downshear quadrants have a mean slope of 1.09, while the two upshear quadrants have a mean slope of 0.38. This difference is statistically significant ( $p = 0.01$ ). For M slope, the USR quadrant is more upright than the other three quadrants ( $p < 0.05$ ), however, the average difference between upshear and downshear is not significant. While individual cases can show significant variation in the slope of the 20 dBZ contour, there is no statistically significant differences in the mean.

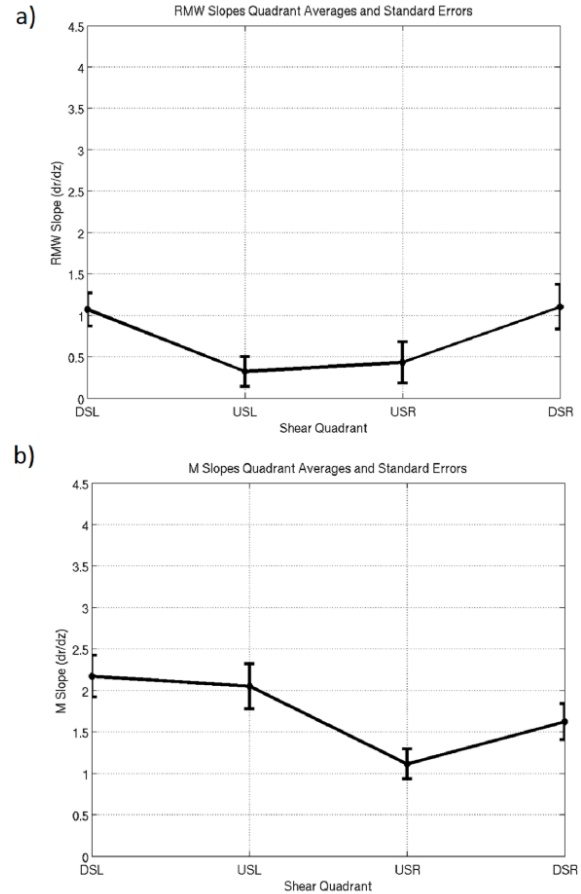


Figure 1: Average slopes and standard errors for the 36 cases for a) RMW slope and b) The slope of an M surface

#### b. Wavenumber-1 Analysis

In order to quantify the wavenumber-1 asymmetry in eyewall slope due to shear, we fit the slopes from each quadrant to a cosine function. The resulting phase and amplitude of the fit provided a measure of the magnitude and direction of the asymmetry due to shear. Figure 2 shows the distribution of the phase for each slope metric. From this figure, we can see that both RMW slope and M slope have a peak in phase downshear, particularly downshear left. This indicates that this asymmetry in slope is a proxy for vortex tilt, which has been shown to be

preferentially downshear-left in the mean (e.g. Reasor et al. 2004, 2013).

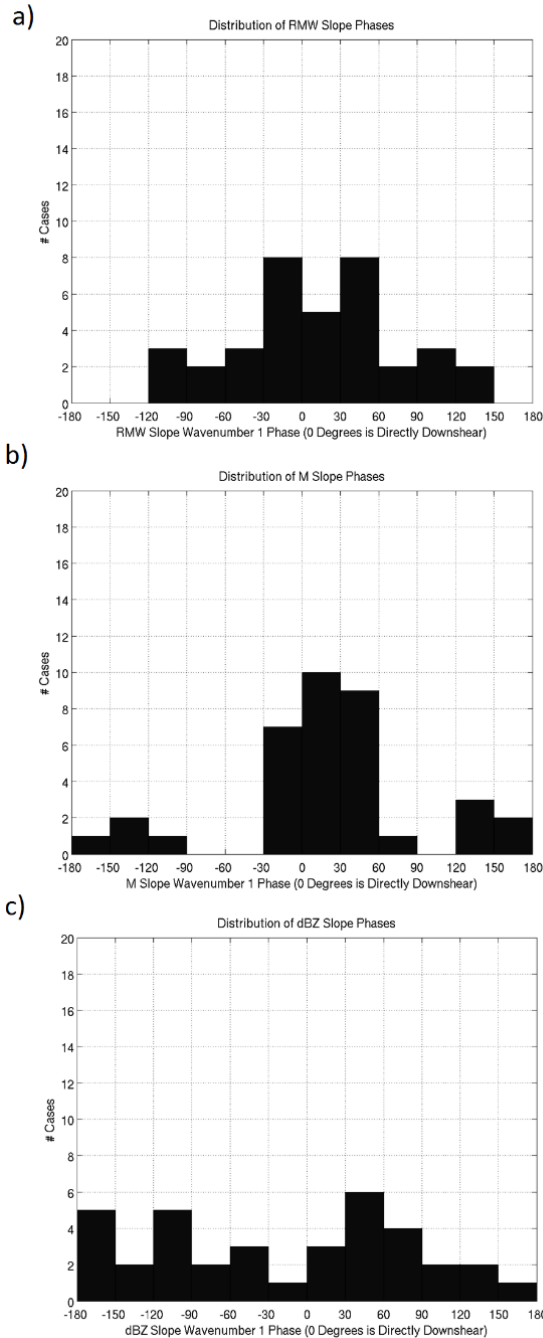


Figure 2: Distribution of the phase of the cosine fit for a) RMW slopes b) M slopes c) 20 dBZ slopes. In each figure, 0 degrees is directly downshear, negative angles are left-of-shear, and positive angles are right-of-shear.

### c. Separation by Shear Magnitude

Next, we compared the cases with high environmental shear (greater than 7 m/s) vs. cases with low environmental shear (less than 2.5 m/s). A statistically significant difference was found in the average amplitude of the wavenumber-1 asymmetries between these two sets for both RMW slope and M slope. This indicates a tendency for the azimuthal variance in eyewall slope to increase as the magnitude of the vertical shear increases. In addition, there was a statistically significant correlation between asymmetry phase and shear magnitude – the asymmetry tended to be more directly downshear as the magnitude of the shear increased, consistent with the notion of a downshear vortex tilt. This is shown for RMW slope in Figure 3 below.

To further illustrate the differences between high shear and low shear cases, composites of the wind data for each quadrant were made for both sets (Figure 4). The slope profiles overlaid on these composite images highlight the tendency for more variation in the high-shear set.

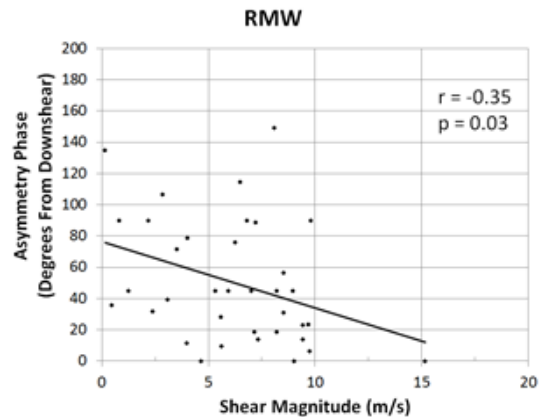


Figure 3: Phase of wavenumber-1 asymmetry (a possible proxy for vortex tilt direction) in RMW slope vs. shear magnitude.

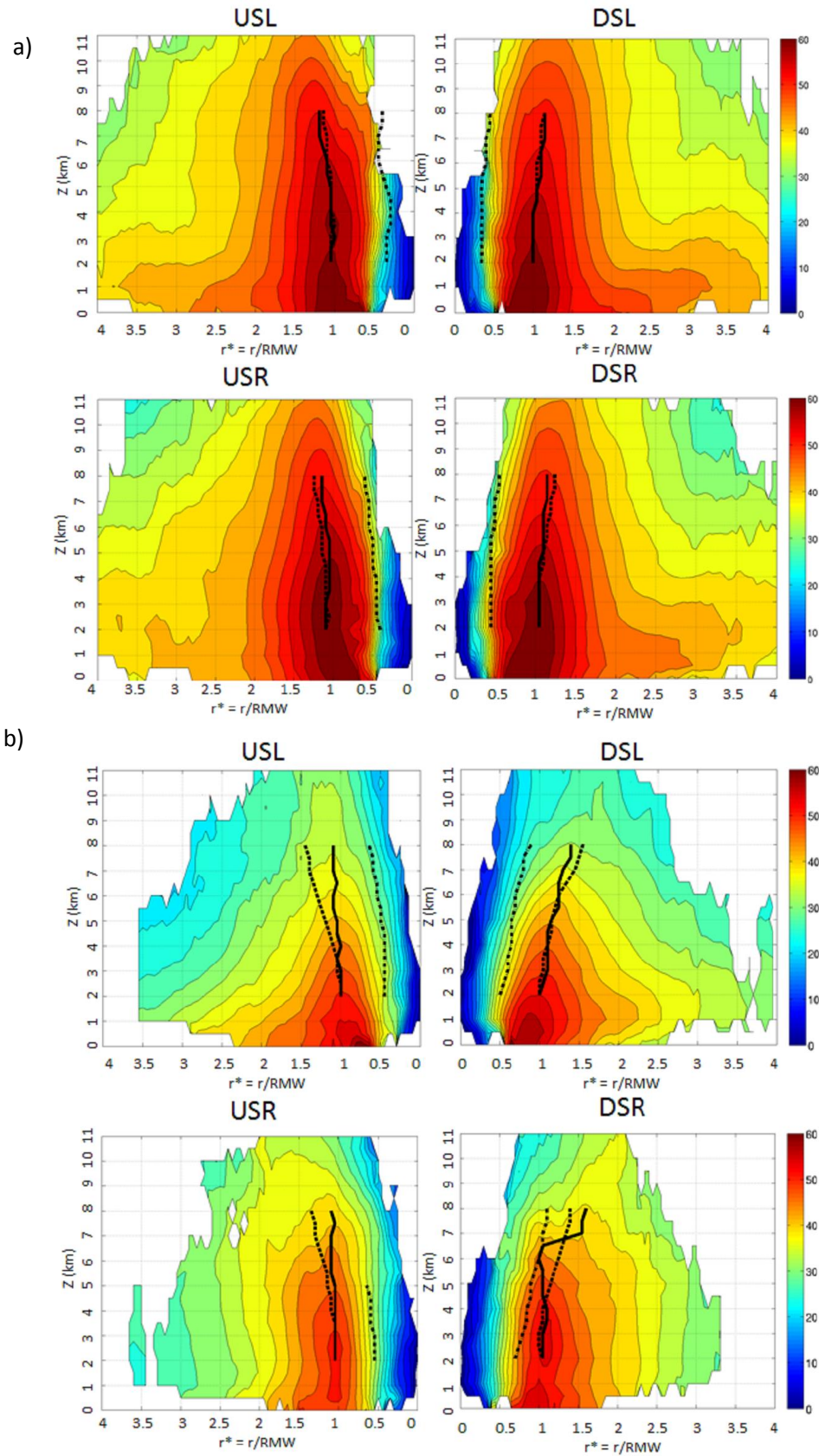


Figure 4: Composites of tangential wind in each quadrant for a) Low-shear and b) High-shear Cases. Also overlaid are the profiles of the RMW (solid), M surface (dashed), and 20 dBZ surface (dot-dashed) used to calculate slope.

*d. Intensifying vs. weakening/steady TCs*

Finally, we compared eyewall slope in intensifying TCs vs. that in weakening/steady TCs, building off of the comprehensive structural comparison in Rogers et al. (2013). Similar to the definition used in that study, intensifying TCs were defined as those where the TC intensified by 10 knots or more in the 12 hours after the observation period.

This was one aspect of the analysis where 20 dBZ slope showed more signal than some of the other metrics. In particular, the 20 dBZ surface was more upright than the M surfaces in the DSL and USL quadrants for intensifying TCs (Figure 5).

**4. SUMMARY AND DISCUSSION**

The two major conclusions of this analysis can be summarized as follows:

1. The shear-relative variation of slope around the eyewall is most pronounced for the RMW and M surfaces. Analysis of the wavenumber-1 asymmetry due to shear show a tendency for greater slope downshear, with the asymmetry increasing as shear magnitude increases, potentially indicating that this slope asymmetry is a proxy for the tilt of the vortex. This is illustrated in Figure 6.
2. The slope of the 20 dBZ surface, as a proxy for the eyewall updraft, is more upright than the slope of the M surface in the left-of-shear quadrants for intensifying TCs, while it is not statistically different for weakening/steady TCs. Since the M surface is bounded to the RMW at  $z = 2$  km, this result indicates convective

heating inside the RMW for intensifying TCs, which, as discussed in Rogers et al. (2013), is a favorable configuration for intensification. This conclusion is summarized in the schematic in Figure 7.

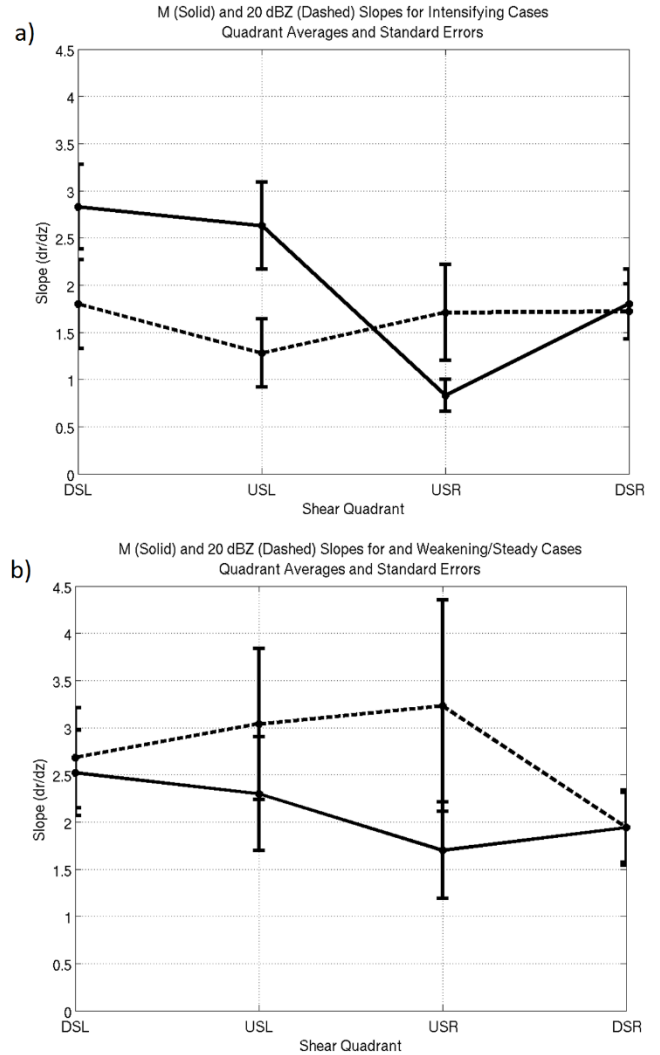


Figure 5: Mean slopes of the 20 dBZ surface (dashed) and M surface (solid) for a) Intensifying cases and b) Weakening/Steady cases.

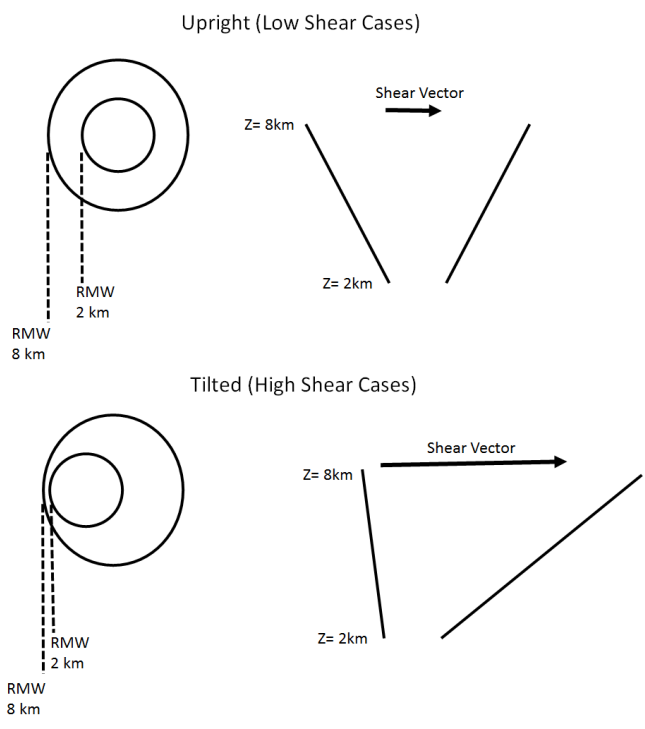


Figure 6: Modeled after Figure 4b of Rogers and Uhlhorn (2008). Schematic illustrating differences in RMW slope variation across the eyewall for low-shear and high-shear TCs.

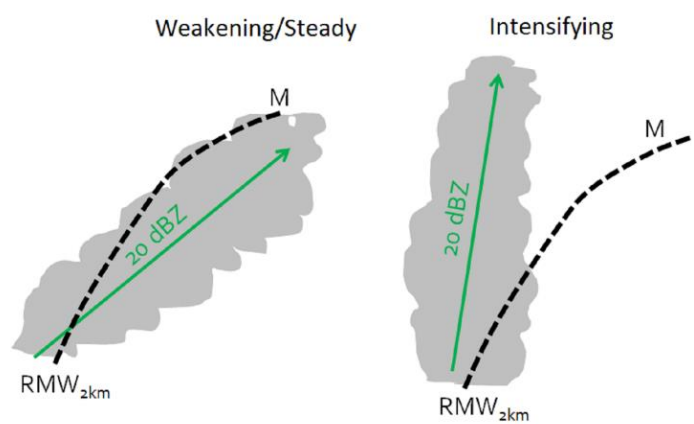


Figure 7: Schematic illustrating the difference between M slope and dBZ slope for intensifying cases and weakening/steady cases.

References:

Bell, M.M., Montgomery, M.T., and W. Lee, 2012: An axisymmetric view of concentric eyewall evolution in Hurricane Rita (2005), *J. Atmos. Sci.*, **69**, 2414-2432.

Black, M.L., Gamache, J.F., Marks, F.D., Samsury, C.E. and H. Willoughby, 2002: Eastern Pacific Hurricanes Jimena of 1991 and Olivia of 1994: The effect of vertical shear on structure and intensity, *Mon. Wea. Rev.*, **130**, 2291-2312.

Chen, H. and D. Zhang, 2013: On the rapid intensification of Hurricane Wilma (2005). Part II: Convective bursts and the upper-level warm core, *J. Atmos. Sci.*, **70**, 146-162.

Chen, S., Knaff, J.A., and F.D. Marks Jr., 2006: Effects of vertical wind shear and storm motion on tropical cyclone rainfall asymmetries deduced from TRMM, *Mon. Wea. Rev.*, **134**, 3190-3208.

Corbosiero, K. L., and J. Molinari, 2002: The effects of vertical wind shear on the distribution of convection in tropical cyclones. *Mon. Wea. Rev.*, **130**, 2110-2123.

—, and —, 2003: The relationship between storm motion, vertical wind shear, and convective asymmetries in tropical cyclones, *J. Atmos. Sci.*, **60**, 366-376.

—, —, and M.L. Black, 2005: The structure and intensification of Hurricane Elena (1985). Part I: symmetric intensification. *Mon. Wea. Rev.*, **133**, 2905-2921.

DeHart, J., Houze, R. and R. Rogers, 2014: Quadrant distribution of tropical cyclone inner-core kinematics in relation to environmental shear, *J. Atmos. Sci.*, in press.

DeMaria, M. and J. Kaplan, 1994: A statistical hurricane intensity prediction scheme (SHIPS) for the Atlantic Basin, *Wea. Forecasting*, **9**, 209-220.

Emanuel, K.A., 1988: The maximum intensity of hurricanes, *J. Atmos. Sci.*, **45**, 1143-1155.

Frank, W.M. and E.A. Ritchie, 2001: Effects of vertical wind shear on the intensity and structure of numerically simulated hurricanes, *Mon. Wea. Rev.*, **129**, 2249-2269.

Gamache, J.F., 1997: Evaluation of a fully three-dimensional variational Doppler analysis technique. Preprints, *28<sup>th</sup> Conf. on Radar Meteorology*, Austin, TX, Amer. Meteor. Soc., 422-423.

- Halverson, J.B., Simpson, J., Heymsfield, G., Pierce, H., Hock, T., and L. Ritchie, 2006: Warm core structure of Hurricane Erin diagnosed from high altitude dropsondes during CAMEX-4, *J. Atmos. Sci.*, **63**, 309-324.
- Hazelton, A.T. and R.E. Hart, 2013: Hurricane eyewall slope as determined from airborne radar reflectivity data: composites and case studies, *Wea. Forecasting*, **28**, 368-386.
- Houze, R.A., F.D. Marks, Jr., and R.A. Black, 1992: Dual-aircraft investigation of the inner core of Hurricane Norbert. Part II: Mesoscale distribution of ice particles. *J. Atmos. Sci.*, **49**, 943-963.
- Jorgensen, D.P., 1984: Mesoscale and convective-scale structure of mature hurricanes. Part I: General observations by research aircraft. *J. Atmos. Sci.*, **41**, 1268-1285.
- Jones, S.C., 1995: The evolution of vortices in vertical shear. I: Initially barotropic vortices, *Quart. J. Roy. Meteor. Soc.*, **121**, 821-851.
- , 2000: The evolution of vortices in vertical shear. III: Baroclinic vortices, *Quart. J. Roy. Meteor. Soc.*, **126**, 3161-3185.
- , 2004: On the ability of dry tropical-cyclone-like vortices to withstand vertical shear, *J. Atmos. Sci.*, **61**, 114-119.
- Kepert, J.D., 2006: Observed boundary layer wind structure and balance in the hurricane core. Part II: Hurricane Mitch, *J. Atmos. Sci.*, **63**, 2194-2211.
- Marks, F.D., 1985: Evolution of the structure of precipitation in Hurricane Allen (1980). *Mon. Wea. Rev.*, **113**, 909-930.
- , and R. A. Houze Jr., 1987: Inner core structure of Hurricane Alicia from airborne Doppler radar observations, *J. Atmos. Sci.*, **44**, 1296-1317.
- NHC, cited 2014: Automated Tropical Cyclone Forecast Archive. [Available online at: <http://ftp.nhc.noaa.gov/atcf/archive/>.]
- Pendergass, A.G. and H.E. Willoughby, 2009: Diabatically-induced secondary flows in tropical cyclones. Part I: Quasi-steady forcing, *Mon. Wea. Rev.*, **137**, 805-821.
- Reasor, P.D., Montgomery, M.T., Marks, F.D. and J.F. Gamache, 2000: Low-wavenumber structure and evolution of the hurricane inner-core observed by airborne Dual-Doppler radar, *Mon. Wea. Rev.*, **128**, 1653-1680.
- , Montgomery, M.T. and L.D. Grasso, 2004: A new look at the problem of tropical cyclones in vertical shear flow: vortex resiliency, *J. Atmos. Sci.*, **61**, 3-22.
- , Rogers, R. and S. Lorsolo, 2013: Environmental flow impacts on tropical cyclone structure diagnosed from airborne Doppler radar composites, *Mon. Wea. Rev.*, **141**, 2949-2969.
- Riemer, M., Montgomery, M.T. and M.E. Nicholls, 2010: A new paradigm for intensity modification of tropical cyclones: thermodynamic impact of vertical wind shear on the inflow layer, *Atmos. Chem. Phys.*, **10**, 3163-3188.
- Rogers, R.F. and E. Uhlhorn, 2008: Observations of the structure and evolution of surface and flight-level wind asymmetries in Hurricane Rita (2005), *Geo. Res. Lett.*, **35**, L22811.
- , F.D. Marks, Jr., and T. Marchok, 2009: Tropical Cyclone Rainfall. In Malcolm G. Anderson (Ed.) *Encyclopedia of Hydrological Sciences*. Chichester, UK: John Wiley & Sons, Ltd. DOI 10.1002/0470848944.hsa030.
- , Lorsolo, S., Reasor, P., Gamache, J. and F. Marks, 2012: Multiscale analysis of tropical cyclone kinematic structure from airborne Doppler radar composites, *Mon. Wea. Rev.*, **140**, 77-99.
- , Reasor, P. and S. Lorsolo, 2013: Airborne Doppler observations of the inner-core structural differences between intensifying and steady-state tropical cyclones, *Mon. Wea. Rev.*, **141**, 2970-2991.
- Shapiro, L. J., and H. E. Willoughby, 1982: The response of balanced hurricanes to local sources of heat and momentum. *J. Atmos. Sci.*, **39**, 378-394.
- Stern, D.P. and D.S. Nolan, 2009: Reexamining the vertical structure of tangential winds in tropical cyclones: observations and theory. *J. Atmos. Sci.*, **66**, 3579-3600.
- , Brisbois, J.R. and D.S. Nolan, 2014: An expanded dataset of hurricane eyewall sizes and slopes, *Mon. Wea. Rev.*, in press.
- Uhlhorn, E.W., B. Klotz, T. Vukicevic, P. Reasor, and R.F. Rogers, 2014: Observed hurricane wind speed asymmetries and relationships to motion and environmental shear. *Mon. Wea. Rev.*, **142**, 1290-1311.
- Willoughby, H.E., Clos, J.A. and M.G. Shoreibah, 1982: Concentric eye walls, secondary wind maxima, and the evolution of the hurricane vortex. *J. Atmos. Sci.*, **39**, 395-411.